CHINESE JOURNAL OF GEOPHYSICS Vol.53, No.6, 2010, pp: 240∼1

JOINT INVERSION OF RECEIVER FUNCTION AND AMBIENT NOISE BASED ON BAYESIAN THEORY

LIU Qi-Yuan[1], LI Yu[1], CHEN Jiu-Hui[1], van der Hilst R. D.[2], GUO Biao[1], WANG Jun[1], QI Shao-Hua[1], LI Shun-Cheng[1]

1 *State Key Laboratory of Earthquake Dynamics, Institute of Geology, CEA, Beijing* 100029*, China*

2 *Department of Earth, Atmospheric and Planetary Science, MIT, Cambridge, MA* 02139*, USA*

Abstract In this study, we present a method for the joint inversion of receiver function and ambient noise based on Bayesian inverse theory (Tarantola, 1987, 2005). The nonlinear inversion method of the complex spectrum ratio of receiver functions (Liu et al., 1996) is extended to perform the joint inversion of the receiver function and ambient noise with a global scanning of the crustal Poisson's ratio. The forward problem of the Rayleigh-wave phase dispersion is solved in terms of a modified version of the fast generalized R/T method proposed by Pei et al. (2008, 2009). Our numerical tests show that (1) the dependency of inversion results on initial models is removed and the model's parameter is estimated reliably even in the case of using a vertically homogeneous model as the initial guess for the crust structure; (2) because the frequency band consistency of the receiver function with the phase dispersion obtained from ambient noise is much better than that with seismic surface waves, the S-wave velocity structure in depth of 0∼80 km can be well estimated by the joint inversion of receiver function and noise-derived phase velocity dispersion in the period range of 2∼40 s, and the space resolution of the shallow structure near to the surface can reach 1 km; (3) global scanning of the Poisson's ratio is not only in favor of data interpretation of the receiver function and ambient noise, but also provides a reliable estimation of the crustal Poisson's ratio. The joint inversion of receiver function and ambient noise recorded at station KWC05 of the western Sichuan seismic array shows that the crustal thickness beneath the station reaches 44 km and the crustal S-wave velocity structure manifests a high-speed upper crust and low-speed middle-lower crust in depth of 24∼42 km. The Poisson's ratio averaged over the crust is 0.262 and that over the low-velocity zone is 0.27.

Key words Joint inversion, Receiver function, Ambient noise, Poisson's ratio, Western Sichuan Array

1 INTRODUCTION

In 1979 Langston[1] proved that under the equivalent seismic source assumption the impulse response (receiver function) of the crust beneath a station can be obtained from the long period teleseismic P waves. On this basis the receiver function method has been developing rapidly, and is widely used in the researches of crust and upper mantle velocity structure. However, there are still controversies on the value of the receiver function inversion method. Based on the result of numerical test Ammon et al.[2] deemed that the inversion result from receiver functions depends on the initial model (non-uniqueness), because receiver functions are sensitive only to the relative information (wave impedance) of the velocity structure. Wu et al.[3] proved that, if appropriate inversion method is adopted, the depths of crustal interfaces and the velocity structure can still be correctly estimated.

As a matter of fact, to evaluate the ability of receiver function method for interpreting realistic data is much more complicated than testing with numerical models. The complexity of crustal structures often renders non-uniqueness to the inversion of receiver function based on one-dimensional model. The nature of geophysical inverse problem determines that some degree of uncertainty is inevitable in its solution, because any observation can constitute a data space of finite dimensions only, while the model parameters to be determined have infinite degrees of freedom[4]. The way to reduce the non-uniqueness is to reduce as many as possible the degrees of freedom of the model parameters. As far as receiver function is concerned, joint inversion combining other independent observations should undoubtedly be the principal developing direction in receiver function studies.

E-mail: qyliu@ies.ac.cn

In fact Özalaybey et al.[5] were the first to develop a linear inversion method combining receiver functions and surface wave phase velocities. Julia et al.[6] further studied the linear damped least squares inversion of receiver function and surface wave group velocity. Sung et al.[7], Lawrence and Wiens[8] developed the nonlinear joint inversion method of receiver functions and surface waves based on the genetic and niching genetic algorithms, respectively. Hu et al.[9] utilized the damped least squares inversion of receiver functions and surface wave group velocities to study the crust and upper mantle velocity structure in the west Yunnan region. Their results indicated that the usage of surface wave data was very effective in constraining the crustal velocity parameters resulting from receiver function inversion. However, the joint inversion requires considering a rather complete period range, therefore, it is necessary to include the surface wave dispersion data of shorter periods in the joint inversion[6]. This means that the joint inversion of receiver functions and surface waves will be restricted to some degree by the seismicity in the study region.

In the recent years the study on ambient seismic noise has made remarkable progress. The studies indicate that, using the cross-correlation method, not only the inter-station Green's function, but also accurate dispersion data of phase or group velocities can be extracted from the diffusive wave field (including ambient noise and scattered coda waves)[10~14]. Even if the unevenness of noise sources is considered, the error of resulting phase velocity could be less than 1%[15]. The result of ambient noise tomography of the west Sichuan array indicated that the phase velocity of period as short as 2 s could be extracted from the ambient noise data observed by a dense array. This means that ambient noise data can not only provide the information of velocity structure on the crustal scale, but also more sufficient constraints on the shallow structure near Earth's surface. Therefore, the joint inversion of receiver function and ambient noise opened a new way for waveform tomography of passive seismic dense arrays.

Theoretically the joint inversion of receiver function and ambient noise is not different in essence from the joint inversion of receiver function and surface wave. However, the current joint inversion of receiver function and surface wave has the following shortcomings. (1) The linear inversion method requires an initial model as close as possible to the real crust, so it is not suitable to the areas lacking preliminary studies. (2) Theoretically the global searching method is useful for averting the inversion from local minima, however, in practice it can not guarantee that the inversion converges to the global optimal solution; more importantly it is very inefficient and is often unacceptable for interpreting the observation data from dense mobile arrays.

To tackle the above problems on the basis of the available method of nonlinear complex spectrum ratio inversion of receiver functions[17], this paper develops a joint inversion technique of receiver function and ambient noise based on the Bayesian inversion theory. It results in a corresponding nonlinear inversion method, and also effectively avoids the inefficient global searching. At the same time we shall adopt a global search of crustal Poisson's ratio in order to get an estimation of the Poisson's ratio of the crust, which has important value for optimizing the fit of the receiver function and surface wave dispersion data derived from ambient noise. We shall start from a brief introduction to the forward calculation algorithm of receiver function and Rayleigh wave phase velocity.

2 FORWARD CALCULATION ALGORITHM

2.1 Receiver Function

The forward calculation of receiver functions and their differential seismograms has a decisive effect on the efficiency of the inversion. In a similar way to literature[17], we adopt the reflectivity method of Müller[18] to calculate the complex spectrum ratio of receiver function. We assume that the incident teleseismic P waves beneath the receiving station are parallel plane waves, so as to avoid the integration over slowness. The reflectivity method of Müller[18] includes iterative recursion of upgoing and downgoing seismic waves, which facilitates the designing of a highly efficient algorithm to calculate receiver function differential seismograms[17~19].

At present the calculations of receiver function from teleseismic P waveform data are mostly based on the equivalent source assumption[1]. Numerical experiments indicated that, for broadband recordings and when

obvious discontinuities exist in the upper part of the receiver region, the vertical component of receiver function can not be simply taken as a -function[17,20]. The easiest way to overcome this difficulty is to use the complex spectrum ratio of radial and vertical receiver functions to replace the original receiver function. Unless specially mentioned, the receiver functions in this paper all refer to the complex spectrum ratio of radial and vertical receiver functions. In fact the receiver functions in complex spectrum domain and in time domain are equivalent. Compared to the inversion of receiver functions in time domain, the inversion in complex spectrum domain avoids repetitive calculations of Fourier transformation, hence reduces the amount of forward calculation of receiver functions (equivalent to data compression). The forward calculation algorithm of receiver functions in complex spectrum domain helps to naturally develop a progressive piecewise inversion method of receiver functions from low to high frequency.

2.2 Forward Calculation of Phase Velocity Dispersion

Most conventional methods for calculating surface wave dispersion are based on the Thomson-Haskell propagation matrix theory[21~24]. Among them the computer code of Herrmann et al.[24] is widely accepted and used. Another kind of methods for calculating surface wave dispersion is the generalized reflection/transmission coefficient (R/T) method developed by Kennett[25] and Luco and Apsel[26]. Although the generalized R/T method has the advantage of numerical stability at all frequencies, its efficiency is relatively low, so it is not very often used in surface wave tomography. To overcome the above drawbacks Chen[27] improved the generalized R/T method to make the theoretical formulas more concise and the method more accurate and stable for high frequencies and thick layers. On this basis Pei et al.[28,29] further developed a fast generalized R/T method for calculating surface wave dispersion. Because the method does not require R/T matrix correction and uses directly the analytic solution of inverse layer matrix, it saves more than 50% of the computing time as compared to the original generalized R/T method[28]. For the joint inversion of receiver function and surface wave, the fast generalized R/T method provided the requisite for building highly efficient computing codes in a unified theoretical frame.

According to literature [28] the phase velocity of surface wave can be obtained by solving the characteristic equation (Note: the characteristic equation in literatures [27,28] contains mistakes)

$$\det(\boldsymbol{E}_{21}^{1}+\boldsymbol{E}_{22}^{1}\Lambda_{\mathrm{u}}^{1}(0)\frown\boldsymbol{R}_{\mathrm{du}}^{1})=0, \tag{1}$$

where det means determinant, $\boldsymbol{E}_{21}^{1}$ and $\boldsymbol{E}_{22}^{1}$ are the submatrices of the first layer matrix of the layered crust model (the upper boundary of the first layer is the ground surface). If $\boldsymbol{E}^{1}$ denotes the matrix of the first layer, then

$$\boldsymbol{E}^{1}=\begin{bmatrix}\boldsymbol{E}_{11}^{1} & \boldsymbol{E}_{12}^{1}\\ \boldsymbol{E}_{21}^{1} & \boldsymbol{E}_{22}^{1}\end{bmatrix}=[e_{lk}]_{4\times4}^{1},$$

where e_{lk} is the elements of layer matrix ($l=1,4;k=1,4$), the superscript indicates the layer number of the crust model, the subscript indicates matrix element. In Eq.(1) $\Lambda_{\mathrm{u}}^{1}(0)$ is the phase delay matrix at zero depth of the first layer, $\frown\boldsymbol{R}_{\mathrm{du}}^{1}$ is the generalized reflection coefficient matrix of the first layer. Here the superscript is the serial number of the crust layer, d and u represent downgoing and upgoing wave, respectively.

The joint inversion of receiver function and surface wave generally involves finely layered crust models (generally the number of layers $N>30$). Therefore, the calculation of layer matrix and its inverse has a large impact on the efficiency of forward calculation of surface wave dispersion. Based on the work of Pei et al.[28], Pan et al.[30] gave out an analytic expression of the inverse of layer matrix in different forms. This paper adopts a different way from the above studies. Based on literature [31] we derived the analytic formulae of layer matrix and its inverse taking the phase velocity as independent variable. For Rayleigh wave the elements of layer matrix can be written as

$$\begin{aligned}&e_{11}=e_{13}=\alpha/c,\quad e_{12}=e_{14}=\beta\nu,\ e_{21}=-e_{23}=\alpha\gamma,\quad e_{22}=-e_{24}=\beta/c,\\&e_{31}=-e_{33}=-2\omega\rho\gamma\alpha\beta^{2}/c,\quad e_{32}=-e_{34}=\omega\rho\chi\beta^{3},\quad e_{41}=e_{43}=\omega\rho\chi\alpha\beta^{2},\quad e_{42}=e_{44}=-2\omega\rho\nu\beta^{3}/c.\end{aligned}$$

The inverse matrix can be written as

$$\boldsymbol{F} = [f_{lk}] = \boldsymbol{E}^{-1}, \tag{2}$$

and we have

$$\begin{aligned} f_{11} =& f_{31} = \alpha^{-1}\beta^2/c, \quad f_{12} = -f_{32} = \chi'/(2c\chi'), \quad f_{13} = -f_{33} = -1/(2\omega\rho\chi'), \quad f_{14} = f_{34} = 1/(2\omega\rho\alpha), \\ f_{21} =& f_{41} = \chi'/(2c\nu'), \quad f_{22} = -f_{42} = \beta/c, \quad f_{23} = -f_{43} = 1/(2\omega\rho\beta 0, \quad f_{24} = f_{44} = -1/(2\omega\rho\nu'), \end{aligned}$$

where α and β is respectively the P and S wave velocity of the layer, ρ is density, c is phase velocity, and ω is the angular frequency. Furthermore

$$\gamma = \sqrt{c^{-2} - \alpha^{-2}}, \quad \gamma' = \sqrt{c^2 - \alpha^2}, \quad \nu = \sqrt{c^{-2} - \beta^{-2}}, \quad \nu' = \sqrt{c^2 - \beta^2}, \quad \chi = \beta^{-2} - 2c^2, \quad \chi' = c^2 - 2\beta^2.$$

For simplicity the layer numbers in above formulas are omitted.

It is easy to find that taking the phase velocity as an independent variable in the formulas of layer matrix and its inverse not only helps to further reduce the calculation amount, but also facilitates the understanding of the relation of phase velocity with layer matrix and its inverse. It is seen from the matrix element of Eq.(2) that when the phase velocity is equal or very close to the S wave velocity of the layer, the inverse of layer matrix will be unstable (it is a price for raising the efficiency of calculation). Therefore, when solving the characteristic Eq.(1) we must prevent such cases from happening. For imperfect elastic medium it is necessary to use complex velocity parameters, which can also effectively avoid the above mentioned instability.

3 JOINT INVERSION OF RECEIVER FUNCTION AND PHASE VELOCITY

The geophysical inverse theory based on the Bayesian theorem was first founded by French Professor Tarantora[31,32]. Bayesian inversion is based on probability theory, which constitutes a theoretical framework for relating the data and the a priori information of the model, so the a priori information can be used to constrain the posterior parameters of the model. This is one of the important reasons for the wide application of the Bayesian inversion theory[31~35]. However, how to establish the a priori probability density function (PDF) of data and model for specific problems is controversial[33,34]. The long-lasting debate has effectively advanced the relevant researches[32].

For the joint inversion of receiver function and ambient noise, the above problem is alleviated to some extent because teleseismic and ambient noise observations afford ample opportunities of repetitive measurements, so the a priori information of data can be realistically estimated. Although the estimation of a priori probability distribution of the model is still a problem to be solved, the usage of ambient noise data reduces greatly the degrees of freedom of the a priori model parameters. For a one-dimensional linear model space (without considering lateral heterogeneous scattering and anisotropy of the crust), we assume that the a priori PDF of observation data and model parameters accords with a normal distribution, which should be a good enough estimation for the concerned problem in the paper.

According to the Bayesian inverse theory[32,33] the posterior probability density of the model space can be expressed as

$$\sigma(\boldsymbol{m}) \propto L(\boldsymbol{m})\rho(\boldsymbol{m}), \tag{3}$$

where $L(\boldsymbol{m})$ is called a likelihood function indicating the fitting degree of model prediction and observation data, $\rho(\boldsymbol{m})$ is the a priori model PDF independent of observation data. In the case of simultaneously considering receiver functions and ambient noise data

$$L(\boldsymbol{m}) \propto \exp\left\{-\frac{1}{2}\left[(\boldsymbol{g}_{\mathrm{RF}}(\boldsymbol{m}) - \boldsymbol{d}_{\mathrm{RF}})\boldsymbol{C}_{\mathrm{RF}}^{-1}(\boldsymbol{g}_{\mathrm{RF}} - \boldsymbol{d}_{\mathrm{RF}}) + (\boldsymbol{g}_{\mathrm{SF}}(\boldsymbol{m}) - \boldsymbol{d}_{\mathrm{SF}})^{\mathrm{T}}\boldsymbol{C}_{\mathrm{SF}}^{-1}(\boldsymbol{g}_{\mathrm{SF}} - \boldsymbol{d}_{\mathrm{SF}})\right]\right\}, \tag{4}$$

and

$$\rho(\boldsymbol{m}) \propto \exp\left[-\frac{1}{2}(\boldsymbol{m} - \boldsymbol{m}_{\mathrm{p}})^{\mathrm{T}}\boldsymbol{C}_{\mathrm{M}}^{-1}(\boldsymbol{m} - \boldsymbol{m}_{\mathrm{p}})\right]. \tag{5}$$

where $\boldsymbol{g}(\boldsymbol{m})$ is the forward calculation operator, $\boldsymbol{d}$ is the vector of observation data, $\boldsymbol{m}$ is the vector of model parameters, $*$ means complex conjugate, T means transposition, subscript RF and SF stands respectively for receiver function and surface wave phase velocity dispersion, subscript p stands for a priori information. $\boldsymbol{C}_{\rm RF}$ and $|pmbC_{\rm SF}$ is the covariance matrix of receiver function and phase velocity dispersion data. $\boldsymbol{C}_{\rm M}$ is the covariance matrix of a priori model.

From Eqs.(4) and (5) we get the corresponding objective function

$$\begin{aligned} S(\boldsymbol{m}) =& \frac{1}{2}\{[\boldsymbol{g}_{\rm RF}(\boldsymbol{m})-\boldsymbol{d}_{\rm RF}]*\boldsymbol{C}_{\rm RF}^{-1}[\boldsymbol{g}_{\rm RF}(\boldsymbol{m})-\boldsymbol{d}_{\rm RF}]+[\boldsymbol{g}_{\rm SF}(\boldsymbol{m})-\boldsymbol{d}_{\rm SF}]*\boldsymbol{C}_{\rm SF}^{-1}[\boldsymbol{g}_{\rm SF}(\boldsymbol{m})-\boldsymbol{d}_{\rm SF}] \\ &+(\boldsymbol{m}-\boldsymbol{m}_{\rm p})^{\rm T}\boldsymbol{C}_{\rm M}^{-1}(\boldsymbol{m}-\boldsymbol{m}_{\rm p})\}. \end{aligned} \tag{6}$$

Solving the inverse problem means to maximize the posterior probability density of model space $\sigma(\boldsymbol{m})$, or in other words, to seek the minimum value of formula (6). Conjugate gradient method is a relatively robust and efficient method for optimizing the objective function $S(\boldsymbol{m})$. The key is how to calculate the gradient of the objective function. From Eq.(6) we get the gradient of objective function

$$\begin{aligned} \gamma_N =& \boldsymbol{C}_{\rm M}\left[\frac{\partial S_\alpha}{\partial m_i}\right]_N = \boldsymbol{C}_{\rm M}\overline{\boldsymbol{RG}}_N^{\rm T}\boldsymbol{C}_{\rm RF}^{-1}{\rm Re}[\boldsymbol{g}_{\rm RF}(\boldsymbol{m})-\boldsymbol{d}_{\rm RF}]+\boldsymbol{C}_{\rm M}\overline{\boldsymbol{IG}}_N^{\rm T}\boldsymbol{C}_{\rm RF}^{-1}{\rm Im}[\boldsymbol{g}_{\rm RF}(\boldsymbol{m})-\boldsymbol{d}_{\rm RF}] \\ &+\boldsymbol{C}_{\rm M}\overline{\boldsymbol{SG}}_N^{\rm T}\boldsymbol{C}_{\rm SF}^{-1}[\boldsymbol{g}_{\rm SF}(\boldsymbol{m})-\boldsymbol{d}_{\rm SF}]+(\boldsymbol{m}_N-\boldsymbol{m}_{\rm p}), \end{aligned} \tag{7}$$

where $\overline{\boldsymbol{RG}}_N = {\rm Re}\left[\frac{\partial g_{\rm RF}^\alpha}{\partial m_i}\right]_N, \overline{\boldsymbol{IG}}_N = {\rm Im}\left[\frac{\partial g_{\rm RF}^\alpha}{\partial m_i}\right]_N, \overline{\boldsymbol{SG}}_N = \left[\frac{\partial g_{\rm SF}^\beta}{\partial m_i}\right]_N$, Re stands for the real part and for imaginary part, subscript N means the Nth iteration; $i=1,2,\cdots,m;\alpha=1,2,\cdots,n;\beta=1,2,\cdots,l$. m,n,l is the layer number of the model and the sample number of receiver function and surface wave dispersion, respectively.

It is known from Eq.(7) that the core in the calculation of the gradient of objective function is to calculate the partial derivatives of receiver function and surface wave dispersion with respect to the model parameters. In the calculation of receiver function differential seismograms we adopted the method of literature [17]. For calculating the partial derivatives of surface wave dispersion with respect to model parameters, there are many methods available, including analytic and numerical. Literatures [31] and [37] gave comprehensive reviews on these subjects. However, the calculation of surface wave partial derivatives is closely related to the corresponding forward calculation algorithm. For the fast generalized R/T method we adopt the implicit function algorithm of Novotiny[38,39]. From the differentiation theorem of implicit functions, for a given period, the partial derivative of surface wave dispersion with respect to the velocity parameters of the model is

$$\overline{\boldsymbol{SG}}_N = \left[\frac{\partial g_{\rm SF}^\alpha}{\partial m_i}\right]_N = -\left[\frac{S'_{m_i}(\boldsymbol{m},c)}{S'_c(\boldsymbol{m},c)}\right]_N, \quad (i=1,2,\cdots,m) \tag{8}$$

where $S(\boldsymbol{m},c)=\boldsymbol{E}_{21}^1+\boldsymbol{E}_{22}^1\mathbb{1}_{\rm u}^1(0)\hat{\boldsymbol{R}}_{\rm du}^1$).

In addition, according to Bayesian inverse theory[32,33] we get the posterior covariance of the model as

$$\boldsymbol{C}'_{\rm M}\approx[\boldsymbol{C}_{\rm M}^{-1}+\overline{\boldsymbol{RG}}^{\rm T}\boldsymbol{C}_{\rm RF}^{-1}\overline{\boldsymbol{RG}}+\overline{\boldsymbol{IG}}^{\rm T}\boldsymbol{C}_{\rm RF}^{-1}\overline{\boldsymbol{IG}}+\overline{\boldsymbol{SG}}\boldsymbol{C}_{\rm SF}^{-1}\overline{\boldsymbol{SG}}]_{m\propto}^{-1}. \tag{9}$$

The spatial resolution can be estimated using the posterior resolution operator

$$\boldsymbol{R}=\boldsymbol{I}-\boldsymbol{C}'_{\rm M}\boldsymbol{C}'^{-1}_{\rm M}. \tag{10}$$

Here $m\propto$ represents the point of maximum likelihood in the model space, $\boldsymbol{I}$ is a unit matrix.

Theoretically, the use of preconditioned conjugate gradient method can accelerate the converging process of inversion[17,32]. However, our practice indicated that for the joint inversion of receiver function and ambient noise the preconditioned conjugate gradient method is not necessary; when the problem is strongly nonlinear and the normal distribution assumption is violated, the preconditioned conjugate gradient method is very likely non-convergent.

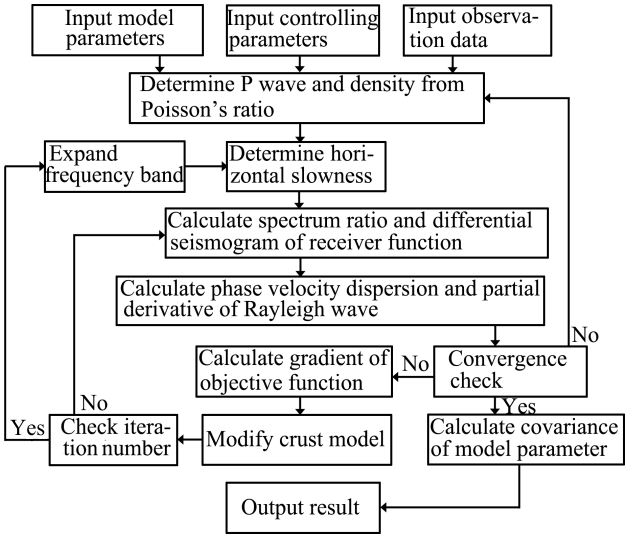

Fig. 1 Diagram for the joint inversion of receiver function and ambient noise

Figure 1 shows the flowchart of the algorithm in this paper. Some explanations to Fig. 1 follow.

(1) As in literature [17] the algorithm of this paper uses the amplitude ratio of the vertical and radial fist arrivals, and includes the receiver function inversions in stepwise expanding frequency bands: 0∼0.5 Hz, 0∼0.75 Hz, 0∼1.0 Hz, 0∼1.25 Hz, and 0∼1.5 Hz. Theory and practice all indicate that it is necessary to include the short period information above 1.0 Hz in receiver function inversion[17]. The lack of short period information above 1.0 Hz is one of the important reasons for the non-uniqueness of the solution.

(2) The algorithm of this paper includes a global searching for Poisson's ratio in the range of 0.2∼0.35 with a freely adjustable step length. However, the modification of Poisson's ratio is restricted in the receiver region of the crust, while the average Poisson's ratio of the crust is calculated by weighted averaging. This means that the average crustal Poisson's ratio given by this paper is an estimation derived under some a priori assumptions. Specifically, the P to S wave speed ratio is set as: 1.8015 in the mantle, 1.74 in the crust when S velocity is greater than 3.57 km/s. When the S wave velocity is less that 2.5 km/s, the P velocity is calculated with the empirical formula $\alpha = 2.1+1.83(\beta-0.7)$. The corresponding density model is calculated by the formula $\rho = 0.32\alpha + 0.77$, where α and β is respectively the velocity of P and S wave. The above assumptions are mainly based on the global models and previous studies, with some adjustments based on our experience. For the joint inversion of receiver function and ambient seismic noise, such a method for estimating average crustal Poisson's ratio is more rational than using a single Poisson's ratio for the entire crust.

(3) The convergence criterion of the inversion is mainly based on the root mean square (rms) error of the fitting of receiver functions and phase velocity dispersion. Obviously the receiver function and phase velocity dispersion have different dimensions. Not only their fitting errors between prediction and observation are different in the order of magnitude, but their converging processes are not coordinated. Therefore we use the following formulas

$$vc = vr/avr + p(vp/avp), \tag{11}$$

and

$$p = (vr \times avp)/(vp \times avr) \tag{12}$$

to estimate the overall variance of the fitting of receiver function and phase velocity dispersion, and take the minimum value of (11) as the criterion of convergence. Formula (12) will be given by the initial value of iteration. vc and vp is the rms fitting error of receiver function and phase velocity dispersion, respectively; while avr and avp is respectively the arithmetic average of observed receiver function amplitude spectra and the observed phase velocities at all periods.

(4) Different from the linear joint inversion of receiver function and surface wave[6], this paper avoids using an artificially specified balance coefficient between receiver functions and surface waves, which is another advantage brought by the Bayesian inverse theory. Owing to the use of data covariance it becomes very easy to assimilate the data of different dimensions. In comparison with other inversion methods, another advantage of Bayesian inverse theory is that the data covariance can coodinates the fitting of data of different reliabilities. This is particularly advantageous to the inversion of receiver functions adopting 1D velocity models.

4 NUMERICAL TEST

Table 1 lists the model of receiver region for numerically testing the method of this paper. In the inversion it is futher refined into a model of 2 km-thick layers. The depth of the crust-mantle boundary is assumed to be 40 km. Outside the receiver region the PREM Earth model is used[40]. We assume that the epicentral distance is 40° and the focal depth is 20 km. The theoretical receiver function and phase velocity dispersion of Rayleigh waves are calculated with the forward calculation algorithm of this paper. The a priori rms error of the receiver function is 1% of the amplitude spectrum, and the a priori rms error of phase velocity at all periods is 0.05 km/s.

Table 1 Model parameters in the receiver area used for the numerical tests

Depth(km)	α(km/s)	β(km/s)	ρ(g/cm3)	Q_α	Q_β	α/β
0	4.401	1.957	2.500	120	60	2.249
2	5.239	3.009	2.500	150	75	1.741
10	6.285	3.612	2.781	200	100	1.740
14	6.803	3.910	2.947	250	125	1.740
20	6.353	3.651	2.803	500	250	1.740
30	6.803	3.910	2.947	600	300	1.740
40	8.121	4.508	3.369	1447	600	1.801
60	7.674	4.260	3.226	1447	600	1.801
80	7.977	4.428	3.323	1447	600	1.801
90	7.846	4.355	3.281	1447	600	1.802
100	7.869	4.368	3.288	1447	600	1.802

Figure 2 shows the testing result. It is seen that in the theoretical model of the receiver region both the crust and the mantle contain low and high velocity layers, and the period range of phase velocities is 3∼30 s. We assume two vertically homogeneous initial models for the receiver region: in the first model $\alpha = 5.239$ km/s,

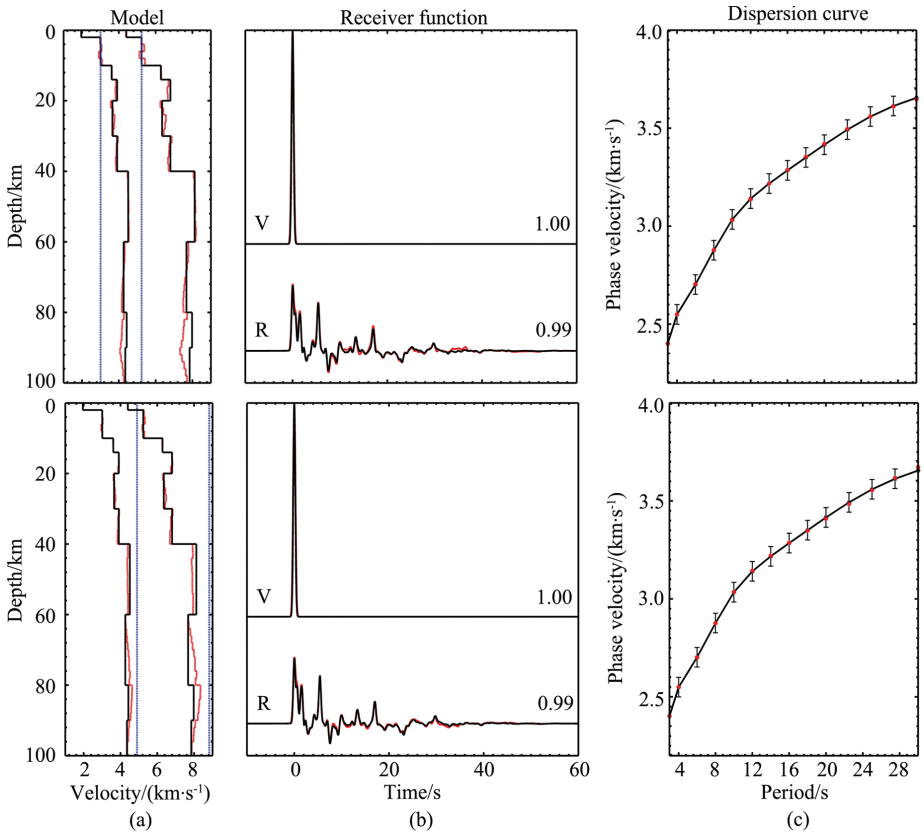

Fig. 2 Numerical tests on the joint inversion of receiver function and ambient noise

(a) Receiver model. Black solid lines represent the P and S velocities of the "true" model; Red dash lines are the inversion model; Blue dot lines are the initial model. (b) Receiver function. Black lines are "true" receiver functions; Red dash lines are the results from inversion; V and R represent the vertical and radial component, respectively. The digits on the right are correlation coefficient. (c) Dispersion curve. Black solid lines with error bars represent the "true" phase dispersion curve of Rayleigh waves (3∼30 s). The red dots are the phase velocity at each period from the inversion.

β = 3.009 km/s, ρ = 2.5 g/cm^3, and in the second model α = 8.82 km/s, β = 4.90 km/s, ρ = 2.5 g/cm^3, where α and β is respectively the P and S wave velocity, and ρ is the density. Although these two initial models are remotely similar to the "true" model, Fig. 2 shows that the velocity model of the receiver region above the depth of 60 km is satisfactorily recovered by the method of this paper. In greater depths, although the error of the predicted model increases with depth, the interface at 80 km can still be correctly inferred.

In order to further examine the impact of phase velocity dispersion on the joint inversion, Fig. 3 shows the numerical testing result for dispersion period 2∼40 s. It is seen from Fig. 3 that the initial model is the "low" velocity model in Fig. 2. Compared to Fig. 2, the resulting velocity structure at depths 60∼80 km is closer to the "true" model parameter, indicating that expanding the dispersion period towards long period helps to constrain the deep structure. In addition, unlike the model in Fig. 2, we used 1 km-thick layers in the top 2 km of the model. Fig. 3 shows that because the dispersion data of period 2 s is used, the inversion method of this paper can predict well the shallow velocity structure. In fact, the numerical testing result indicated that, when the dispersion data is limited above 3 s, the near-surface structure from inversion is nonunique, because in

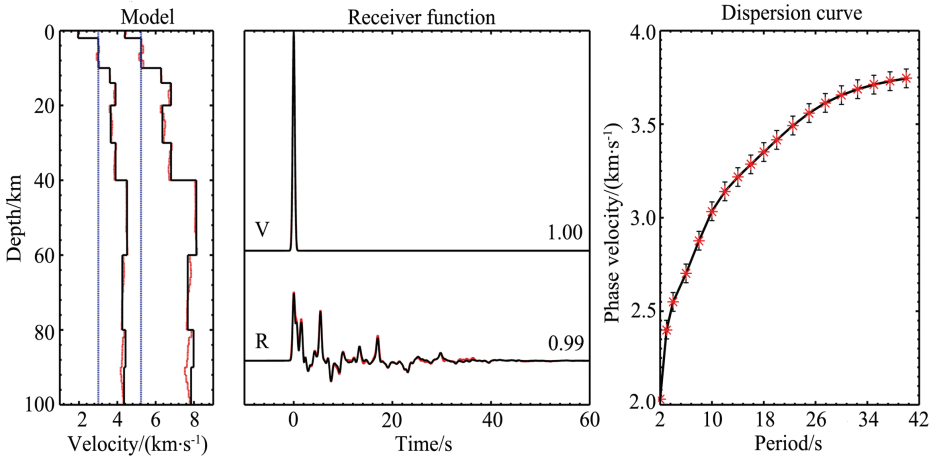

Fig. 3 Numerical tests on the joint inversion of receiver function and ambient noise. The notation used is same with those in Fig. 2.

such case neither the receiver function nor the surface wave data can strictly constrain the shallow structure. This result has important reference value for the interpretation of practical observation data.

Figure 4 shows the variation of fitting error of receiver function and Rayleigh wave phase velocities with crustal Poisson's ratio. The initial model used in the inversion is the "high" velocity model in Fig. 2. Fig. 4 shows that for both the receiver function and phase velocity dispersion the fitting error of predicted and observed data has a single minimum. The average crustal Poisson's ratio from the inversion is 0.2648, while that of the "true" model (Table 1) is 0.2639, the relative error is about 0.3%.

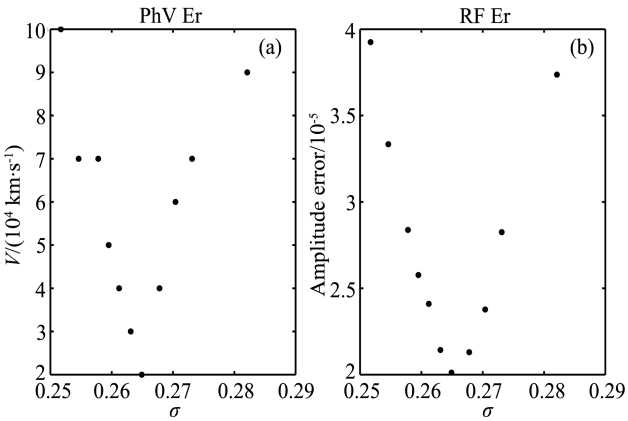

Fig. 4 Variations of fitting errors of the phase velocity (a) and receiver function (b) with the average Poisson's ratio of the crust

5 EXAMPLE OF APPLICATION

During 2006∼2009 the State Key Laboratory of Earthquake Dynamics, Institute of Geology, CEA deployed a dense mobile broadband seismograph array (hereinafter called West Sichuan Array for brevity) consisting of 297 stations in west Sichuan (26°N∼32°, 100°E∼105°E)[41]. Liu et al.[42] have used the receiver function method

to study the crust and upper mantle velocity structure beneath the West Sichuan Array stations along latitude 31°N. Li et al.[16] have given the surface wave tomography result from the ambient noise recorded by West Sichuan Array. These provided a basis for us to test our method. We shall directly use their result. For the processing of ambient noise data refer to literature [16].

As an example we use the inversion method of this paper to restudy the crust and upper mantle S-wave velocity structure within depth range 0∼100 km beneath station KWC05 of the West Sichuan Array (located at 31°N). Fig. 5 shows the time-domain receiver functions in different azimuths at station KWC05. Unlike literature [42] the receiver functions in Fig. 5 are derived from the P waveforms of 55 distant earthquakes with the iterative deconvolution method[43]. The epicentral distance range is 35°∼60°; station azimuth is 46°∼207°. It should be mentioned that the receiver functions in Fig. 5 resulted from stacking in azimuthal groups. In each receiver function group the azimuth variation was restricted within 1 degree. The grouped stacking of receiver functions helps to suppress the scattering caused by lateral heterogeneity in different azimuths with equal weights.

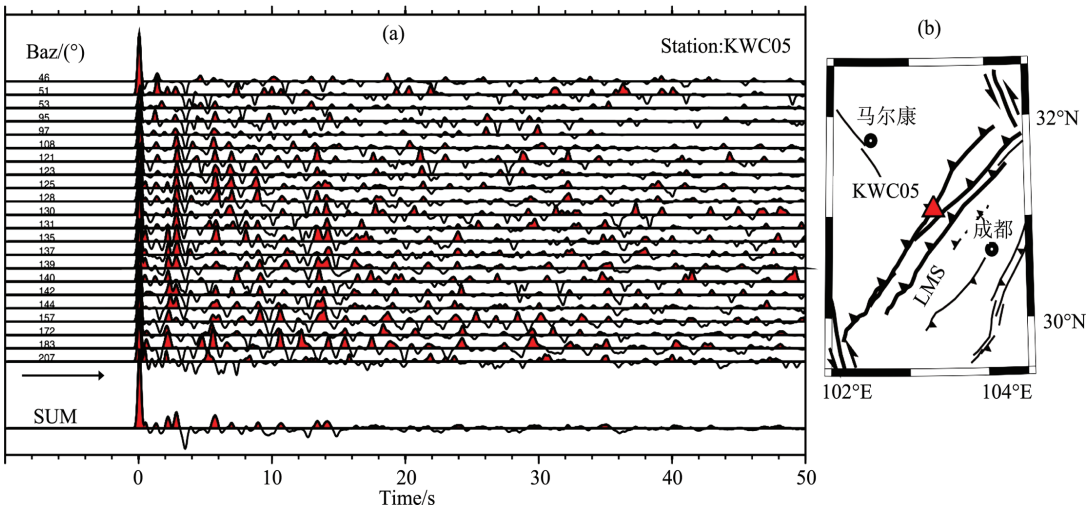

Fig. 5 Receiver functions at station KWC05 in different azimuths

(a) Receiver function; Baz denotes the back azimuth (°); SUM denotes the summation over azimuths.

(b) Station map; LMS denotes the Longmen Shan faults.

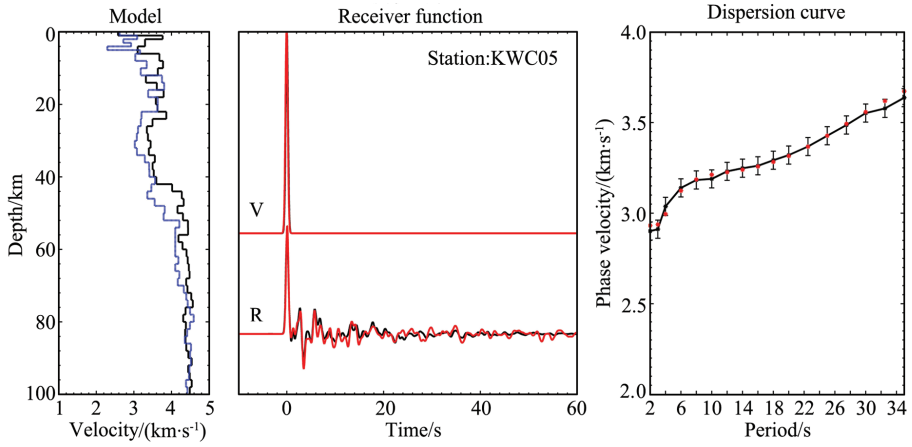

Fig. 6 Inversion of the crust and upper mantle velocity structure beneath station KWC05

The notations are the same as those in Fig. 2. The period of the phase dispersion of ambient noise is 2∼35 s.

Left panel: the black solid line shows the crust and upper mantle velocity structure by the joint inversion, and blue dash line shows that obtained by the receiver function inversion.

Figure 6 gives the inversion result of this paper. It shows that both the receiver function and the ambient noise data are well interpreted. The S wave velocity structure beneath station KWC05 indicates that the crustal thickness is 44 km, the upper crust is a high velocity structure, while the middle and lower crust between depths 24∼42 km is a relatively low velocity zone. Our re-interpretation indicates that the average crustal Poisson's ratio beneath station KWC05 is 0.262, and the Poisson's ratio of the low velocity zone in the crust is 0.270. Fig. 6 also shows the S wave velocity structure resulted from non-linear receiver function complex spectrum ratio inversion[42]. A comparison reveals obvious differences between the two results. Therefore it is inferred that the phase velocity dispersion data from the ambient noise played an important role in constraining the absolute S-wave velocity of the crust and topmost mantle. In fact, in the cases of inversion with receiver functions alone, the only criterion for judging the inversion result is the fitness of receiver function waveforms, whereas the impact of medium lateral variation on the receiver function can not be considered.

6 DISCUSSION AND CONCLUSION

On the basis of the available inversion method of nonlinear complex spectrum ratio of receiver functions[17], this paper further developed a joint inversion method of receiver function and ambient noise based on the Bayesian inverse theory. The results of numerical tests and interpretation of real data lead to the following conclusions.

(1) The inversion result produced by the method of this paper is independent of the initial model. Even if there is only a very crude estimation of the crustal structure beneath the station, our method can still make very good prediction to the model parameters, indicating that the phase velocity dispersion data provide powerful constraints on the absolute S-wave velocity of the crust. Therefore, for the joint inversion of ambient noise and receiver function, the global searching method is not absolutely necessary.

(2) The method of this paper can equally be used for the joint inversion of seismic surface wave and receiver function. However, because ambient noise can provide surface wave dispersion data in the frequency range approximately the same as receiver functions, the joint inversion of ambient noise and receiver function can better constrain the crust and upper mantle, especially the near-surface velocity structure beneath the station. When the period range of phase velocity dispersion from ambient noise is 2∼40 s, the joint inversion of ambient noise and receiver function can reliably predict the S wave velocity structure in the depth range of 0∼80 km beneath the station, and the resolution for shallow structure can reach 1 km.

(3) The method of this paper differs from the existing joint inversion method for surface wave and receiver function, as it carries out a global searching for the crustal Poisson's ratio. In this way we can not only interpret the receiver function and surface wave dispersion data from ambient noise more rationally, hence improve the fitting quality to the data, but also obtain an estimation of the Poisson's ratio of the crust under some a priori assumptions.

(4) The joint inversion result of the observation data from station KWC05 of the West Sichuan Array indicates that the crust beneath the station is 44 km thick, the upper crust has obviously high velocity, and the middle and lower crust in the depth range 24∼42km has low velocity. The average Poisson's ratio of the crust is 0.262, and that of the intra-crust low velocity zone is 0.270.

(5) When the crustal structure contains low velocity layers the attenuation parameter of the medium has an important impact on the joint inversion of ambient noise and receiver function. In the interpretation of real data a simple trial method was used to estimate the attenuation parameter of the medium. In principle there is no difficulty in using the present method to simultaneously invert further for the attenuation parameter of the medium.

(6) The joint inversion of ambient noise and receiver function is obviously superior to the inversion of receiver function alone, and also superior to the joint inversion of surface wave and receiver function. However, as it is restricted by the observation conditions of ambient noise, the method is mainly suitable for studying the fine velocity structure of crust and upper mantle beneath a dense seismograph network or array.

ACKNOWLEDGMENTS

The research was supported by the National Natural Science Foundation of China ( )

REFERENCES

[1] Langston C A. Structure under Mount Rainier, Washington, inferred from teleseismic body waves. *J. Geophys. Res.*, 1979, **84**: 4749∼4762

[2] Ammon C J, Randall G, Zandt G. On the nonuniqueness of receiver function inversions. *J. Geophys. Res.*, 1990, **95**(B10): 15303∼15318

[3] Wu Q, Li Y, Zhang R, et al. Wavelet modeling of broad-band receiver functions. *Geophys. J. Int.*, 2007, **170**(2): 534∼544

[4] Scales J A, Snieder R. The anatomy of inverse problems. *Geophysics*, 2000, **65**(6): 1708∼1710

[5] Özalaybey S, Savage M K, Sheehan A F, et al. Shear-wave velocity structure in the northern Basin and Range province from the combined analysis of receiver functions and surface waves. *Bull. Seism. Soc. Am.*, 1997, **87**(1): 183∼199

[6] Julia J, Ammon C J, Herrmann R B, et al. Joint inversion of receiver function and surface wave dispersion observations. *Geophys. J. Int.*, 2000, **143**(1): 1∼19

[7] Sung J C, Chang-Eob B, Langston C A. Joint analysis of teleseismic receiver functions and surface wave dispersion using the Genetic algorithm. *Bull. Seism. Soc. Am.*, 2004, **94**(2): 691∼704

[8] Lawrence J F, Wiens D A. Combined receiver-function and surface wave phase-velocity inversion using a niching genetic algorithm: application to Patagonia. *Bull. Seism. Soc. Am.*, 2004, **94**(3): 977∼987

[9] Hu J F, Zhu X G, Xia J Y, et al. Using surface wave and receiver function to jointly inverse the crust-mantle velocity structure in the West Yunnan area. *Chinese J. Geophys.* (in Chinese), 2005, **48**(5): 1069∼1076

[10] Lobkis O I, Weaver R L. On the emergence of the Green's function in the correlations of a diffusive field. *J. acoust. Soc. Am.*, 2001, **110**(6): 3011∼3017

[11] Weaver R L, Lobkis O I. Diffuse fields in open systems and the emergence of the Green's function. *J. acoust. Soc. Am.*, 2004, **116**(5): 2731∼2734

[12] Campillo M, Paul A. Long-Range correlations in the diffuse seismic coda. *Science*, 2003, **299**(5606): 547∼549

[13] Shapiro N M, Campillo M. Emergence of broadband Rayleigh waves from correlations of the ambient seismic noise. *Geophys. Res. Lett.*, 2004, **31**(7): 1615∼1619

[14] Shapiro N M, Campillo M, Stehly L, et al. High-resolution surface-wave tomography from ambient seismic noise. *Science*, 2005, **307**: 1615∼1618

[15] Yao H J, van der Hilst R D. Analysis of ambient noise energy distribution and phase velocity bias in ambient noise tomography, with application to SE Tibet. *Geophys. J. Int.*, 2009, **179**(4): 1113∼1132

[16] Li Y, Yao H J, Liu Q Y, et al. Phase velocity array tomography of Rayleigh waves in western Sichuan from ambient noise. *Chinese J. Geophys.* (in Chinese), 2010, **53**(4): 842∼852

[17] Liu Q Y, Kind R, Li S C. Maximal likelihood estimation and nonlinear inversion of the complex receiver function spectrum ratio. *Chinese J. Geophys.* (in Chinese), 1996, **39**(4): 502∼513

[18] Müller G. The reflectivity method: a tutorial. *J. Geophys.*, 1985, **58**(3): 153∼174

[19] Randall G E. Efficient calculation of differential seismograms for lithospheric receiver functions. *J. Geophys. Int.*, 1989, **99**(3): 469∼481

[20] Scherbaum F. Seismic imaging of the site response using micro-earthquake recordings, part I: method. *Bull. Seism. Soc. Am.*, 1987, **77**: 1905∼1923

[21] Thomson W T. Transmission of elastic waves through a stratified solid medium. *J. Appl. Physics*, 1950, **21**(2): 89∼93

[22] Haskell N A. The dispersion of surface waves on a multi-layered medium. *Bull. Seism. Soc. Am.*, 1953, **43**(1): 17∼34

[23] Dunkin J W. Computation of modal solution in layered, elastic media at high frequencies. *Bull. Seism. Soc. Am.*, 1965, **53**(2): 335∼358

[24] Herrmann R B, Ammon C J. Computer programs in seismology version 3.20: Surface waves, receiver functions, and crustal structure. St. Louis University, Missouri. 2002, Available at http://mnw.eas.slu.edu/ People/RBHerrmann

[25] Kennett B L N. Seismic Wave Propagation in Stratified Media. Cambridge University Press, 1983
[26] Luco J E, Apsel R J. On the Green's function for a layered half-space, part I. *Bull. Seism. Soc. Am.*, 1983, **73**(4): 909∼929
[27] Chen X. A systematic and efficient method of computing normal modes for multilayered half-space. *Geophy. J. Int.*, 1993, **115**(2): 391∼409
[28] Pei D H, John N L, Pullammanappallil S K, et al. Improvements on computation of phase velocities of Rayleigh waves based on the generalized R/T coefficient method. *Bull. Seism. Soc. Am.*, 2008, **98**(1): 280∼287
[29] Pei D H, John N L, Pullammanappallil S K, et al. Erratum to improvements on computation of phase velocities of Rayleigh waves based on the generalized R/T coefficient method. *Bull. Seism. Soc. Am.*, 2009, **99**(4): 2610∼2611
[30] Pan J T, Wu Q J, Li Y H. Group velocities computation of surface waves based on the fast generalized R/T coefficient method. (in Chinese), 2009, **24**(6): 2030∼2035
[31] Aki K, Richards P G. Quantitative Seismology, Second Ed. University Science Books, Sausalito, Californian, 2002
[32] Tarantola A. Inverse Problem Theory, Methods for Data Fitting and Model Parameter Estimation. Elsevier, Amsterdam, 1987
[33] Tarantola A. Inverse Problem Theory, and Methods for Model Parameter Estimation. SIAM, PA 19104-2688 USA, 2005
[34] Scales J A, Snieder R. To Bayes or not to Bayes. *Geophysics*, 1997, **62**(4): 1045∼1046
[35] Gouveia W P, Scales J A. Bayesian seismic waveform inversion: parameter estimation and uncertainty analysis. *J. Geophys. Res.*, 1998, **103**(2): 2759∼2779
[36] Gao S. A Bayesian nonlinear inversion of seismic body-wave attenuation factors. *Bull. Seism. Soc. Am.*, 1997, **87**(4): 961∼970
[37] Cercato M. Computation of partial derivatives of Rayleigh-wave phase velocity using second-order subdeterminants. *Geophys. J. Int.*, 2007, **170**(1): 217∼238
[38] Novotiny O. Partial derivatives of dispersion curves of Love waves in layered medium. *Studia Geoph. et Geod.*, 1970, **14**(1): 36∼50
[39] Novotiny O. Methods of computing the partial derivatives of dispersion curves. *Pure. Appl. Geophys.*, 1976, **114**(5): 765∼775
[40] Dziewonski A M, Anderson D L. Preliminary reference Earth model. *Phys. Earth Planet. Int.*, 1981, **25**(4): 297∼356
[41] Liu Q Y, Chen J H, Li S C, et al. The M_s8.0 Wenchuan earthquake: Preliminary results from the western Sichuan mobile seismic array observations. *Seismology and Geology* (in Chinese), 2008, **30**(3): 584∼596
[42] Liu Q Y, Li Y, Chen J H. Wenchuan M_s8.0 earthquake: S-wave velocity structure of the crust and upper mantle. *Chinese J. Geophys.* (in Chinese), 2009, **52**(2): 309∼319
[43] Ligorria J P, Ammon C J. Iterative deconvolution of teleseismic seismograms and receiver function estimation. *Bull. Seism. Soc. Am.*, 1999, **89**(5): 1395∼1400